Contents lists available at ScienceDirect

Forest Ecology and Management

Stand density effects on carbon and water fluxes in a semi-arid forest, from leaf to stand-scale

Mor Tsamir[a], Sagi Gottlieb[b], Yakir Preisler[b], Eyal Rotenberg[b], Fyodor Tatarinov[b], Dan Yakir[b], Christina Tague[c], Tamir Klein[a],*

[a] *Plant & Environmental Sciences Department, Weizmann Institute of Science, Rehovot, Israel*
[b] *Earth and Planetary Science Department, Weizmann Institute of Science, Rehovot, Israel*
[c] *Bren School of Environmental Science & Management, University of California, Santa Barbara, CA, USA*

ABSTRACT

Drought-induced productivity reductions and tree mortality have been increasing in recent decades in forests around the globe. Prescribed reduction in stand density, i.e. thinning, has been proposed as a management tool to improve forest sustainability in face of a warmer, drier future. Thinning should potentially reduce net stand water use and improve water-availability for remaining trees, thus reducing their subsequent drought vulnerability. However, few studies have directly measured these effects.

In 2009 we established a large-scale thinning experiment in a semi-arid, 40-years-old pine afforestation. Study plots (70 × 70 m) were thinned to 100, 200, and 300 trees ha^{-1}, and compared with unthinned control plots (210–400 trees ha^{-1}), each at five replications. Stem and needle growth, and needle gas exchange were measured along 3–9 consecutive years at seasonal to annual temporal resolution. Measurements at the tree-scale were further up-scaled using both simple upscaling relationships and using an ecosystem model of coupled carbon, energy and hydrology (Regional Hydro Ecologic Simulation System, RHESSys).

At the needle scale, photosynthesis was 70% higher at the 100 trees ha^{-1} than at 300 trees ha^{-1}, whereas transpiration was merely 10% higher. Consequently, stem and needle growth increased by 100% and 20%, respectively. For most parameters, there was little change between 200 and 100 trees ha^{-1}. Applying RHESSys at the stand-scale, these effects on tree physiology translated into 35% reduction in CO_2 uptake and a 47% reduction in tree water-use, which was compensated for by increased evaporation from exposed soil.

Our long-term measurements at the dry timberline highlight the role of thinning in enhancing the activity and growth of remaining trees, with increased water-use efficiency. Unexpectedly, this density reduction was associated with a relatively small decrease in forest carbon uptake. Light availability was a limiting factor in the higher density plots, even in our light-abundant forest.

1. Introduction

Drought-induced tree mortality has been increasing in recent decades in forests around the globe, following the warming climate (Klein and Hartmann, 2018). Semi-arid forests are under a bigger threat since these drought episodes, which are typical to these areas, are expected to be more frequent due to climate change (Moreno and Cubera, 2008; Clark et al., 2016; Preisler et al., 2019). Even considering the better drought acclimation of tree species in semi-arid forests compared with more mesic species (Helman et al., 2017), the fact that most semi-arid forests are at the borderline of tree existence puts them in higher risk (Klein et al., 2015). Prescribed reduction in stand density, i.e. thinning,

has been proposed as a major management tool to improve forest sustainability in face of a warmer and drier future (McDowell and Allen, 2015). It has been suggested that reducing stand density through sustainable harvesting can increase the resilience of forests to drought, (McDowell and Allen, 2015) as well as improve forest productivity, carbon sequestration and in some case increase groundwater recharge and ultimately streamflow (Tague et al., 2019).

Forest thinning alters both light and water availability (Goodwin et al., 2018). While thinning directly reduces the water interception and transpiration associated with removed vegetation, there are numerous compensating mechanisms. Light availability at the ground surface is increased by thinning and field studies have found both an increase in
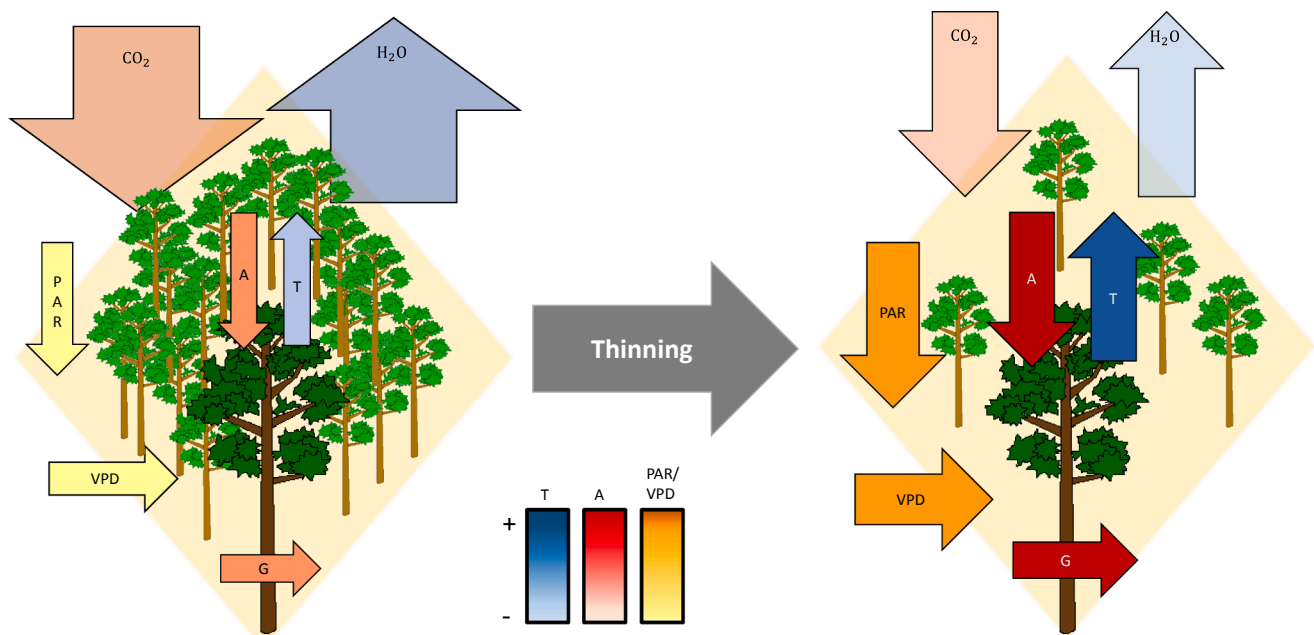
Fig. 1. Conceptual scheme for the expected changes of forest thinning on major tree and stand water, carbon, and energy fluxes. The decrease in stand density should increase the photosynthetically active radiation (PAR) below the canopy and vapor pressure deficit (VPD). As a result, tree-scale carbon assimilation (A), transpiration (T), and growth (G) should increase respectively. This tree-scale intensification would not scale to the stand level CO_2 uptake and water-use due to the lower number of trees.

light penetration and soil temperature following thinning (Bréda et al., 1995; Simonin et al., 2007). As a result, evaporation from the litter and soil surface (E_s) is amplified in thinned stands (Raz-Yaseef et al., 2010a, 2010b; Moreno and Cubera, 2008), potentially causing diminution in water availability for remaining trees. Similarly, in areas with substantial understory vegetation, understory growth and transpiration may be increased following thinning (Vesala et al., 2005; Nunes et al., 2014). However, we note that semi-arid forests are typically poor in understory vegetation, partly due to a short growth period during the wet season (Grünzweig et al., 2003). On the other hand, during the wet season, reduced interception losses and reduced transpiration with density reduction may lead to increases in infiltration of water to the soil, in turn increasing water availability for tree water-use in remaining trees (Raz-Yaseef et al., 2010a, 2010b). In warm semi-arid regions, the common assumption is that temporal and spatial variation in water availability has greater impact on stand growth than, e.g., light intensity (Rotenberg and Yakir, 2010; Moreno-Gutiérrez et al., 2011; Olivar et al., 2014; Klein et al., 2015; Giuggiola et al., 2016). Tree-scale water availability is also influenced by ecophysiology including root distribution and species-specific differences in stomatal function. Studies have shown that thinning-induced changes in soil water availability exert many impacts on the forest, including decreased leaf area index and transpiration at the stand scale, and increased cambial growth of remaining trees (Bréda et al., 1995; Olivar et al., 2014; Del Campo et al., 2014; Calev et al., 2016). In addition to the short-term thinning effects on water, light, and gas exchange parameters, subsequent changes to forest structure and composition can result in multi-year impacts that evolve over time. For example, thinning can increase the understory vegetation density, due to the reduction of competition over resources (Nunes et al., 2014).

Field studies that have measured post-density reduction impacts, including intentional managed density reduction and reduction related to natural disturbances such as mortality, remain relatively few. Available studies have shown a diversity of thinning-induced changes including both increases and decreases in stand-scale transpiration (Bréda et al., 1995; Olivar et al., 2014; Del Campo et al., 2014; Calev et al., 2016; Clark et al., 2016). While previous studies have shown that

thinning enhances tree-scale carbon assimilation and cambial growth in the remaining trees (Olivar et al., 2014; Moreno-Gutiérrez et al., 2011; Navarro-Cerrillo et al., 2016), a smaller number of studies examined effects at the stand-scale. The few existing studies indicate that at the stand-scale, thinning reduced carbon uptake capacity due to the reduction in stand density (Delas Heras et al., 2013). It is unknown whether the increase in tree-scale photosynthesis can compensate for the reduction in tree number and therefore maintain the forest role in carbon sequestration as part of the global carbon cycle. Further, estimation of thinning impacts across the diversity of site conditions within semi-arid regions is still needed to assess the generalizability of individual experiments. This study is designed to address this need. Our previous research in the semi-arid pine forest, examined in this study, indicated that net ecosystem exchange (NEE) was unexpectedly high in comparison to forests in mesic areas, despite the lower precipitation (Grünzweig et al., 2003). Assessing the response of this semi-arid forest, located at the dry timberline, is designed to provide insight into thinning responses in the most drought-exposed forest sites, which are at higher risk (Klein et al., 2014b; McDowell and Allen, 2015).

Based on previous studies of forest thinning effects and expected interactions between the canopy parameters described above, we hypothesized that thinning in a semi-arid forest should induce the following inter-related, cascading impacts on water, carbon, and energy fluxes (Fig. 1): thinning should cause an increase in both below canopy photosynthetically active radiation (PAR) and vapor pressure deficit (VPD). For remaining trees, tree-scale carbon assimilation (A), transpiration (T), and growth (G) should also increase. On the other hand, at the stand-scale, these tree scale increases in A and T will be compensated by reductions in A and T due to the loss of trees. Therefore, following thinning we expect stand level CO_2 uptake and water-use to be similar or lower compared to the unthinned state. Here we test the hypotheses above by a large-scale thinning experiment in a semi-arid pine afforestation. Study plots were thinned to 100, 200, and 300 trees ha^{-1}, each with five replications. Unthinned control plots were used to test any bias related to thinning stress (thinning-induced inhibition of tree growth; Peltola et al., 2002; Pukkala et al., 2002; Di Matteo et al., 2010; Kariuki, 2008). Stem diameter increment, needle length, and

needle gas exchange were measured along 3–9 consecutive years at seasonal to annual temporal resolution. Measurements at the tree-scale were further up-scaled using simple scaling relationships, which have been established in previous studies such as leaf area index (Sprintsin et al., 2007, 2011). Finally, up-scaling was performed using a process-based ecohydrology model (RHESSys) that has been used in previous studies to estimate stand to forest scale carbon and water fluxes (Tague and Band, 2004; Zierl et al., 2007; Tague et al., 2013; Saksa et al., 2017).

2. Materials & methods

2.1. Site and climate

Our study was conducted in Yatir forest, about 50-years-old *Pinus halepensis* plantation located at the northern edge of the Negev desert, Israel (31°20′N, 35°20′E; Figs. S1–S2). The climate is hot and dry (40-year average annual temperature and precipitation are 18.2 °C and 285 mm). Stand density is ca. 300 trees ha^{-1}, mean tree height is 10.2 ± 2.5 m and mean diameter at breast height (DBH) is 19.8 ± 5.6 cm. In 2000, an instrumented flux tower that is part of a Global FluxNet (https://fluxnet.ornl.gov/) was erected in the geographic center of the forest, allowing continuous measurements of NEE and GPP (Grünzweig et al., 2003; Rotenberg and Yakir, 2010).

2.2. Thinning experiment

During autumn 2009 twenty-one forest plots (of about 70 × 70 m) were thinned to three stand density levels: 100, 200, and 300 trees ha^{-1} (Fig. S1c); Four unthinned plots (220–400 trees ha^{-1}) were left for control. For convenience, stand densities are expressed in the text in trees ha^{-1}. Tree felling was done on pre-marked trees, to produce plots with evenly distributed, healthy trees. Within each plot, 30 m long parallel transects were located 20 m from the plot edge, to ensure a buffer zone, limiting impacts from conditions beyond the plot edge. Along these transects, woody vegetation growth and seedling germination were monitored annually. Tree measurements such as stem diameter increment, needle length and needle gas exchange (see Table 1 for a complete list of parameters) were done on 7 trees at each plot, selected randomly from the 4 corners of the plot (2 trees from 3 corners and 1 tree from 1 corner), for a total 147 selected trees. All trees were measured for stem growth and needle length in 2010–2017, and 5 trees from each of 4 plots were measured for leaf gas exchange, PAR and VPD in 2010–2012. The study of grazing effects was conducted in 15 of the plots, as part of another research project, which is not reported here.

2.3. Stem and needle growth

In 2010, manual steel band dendrometers were installed at 1.5 m above ground to measure stem growth. Dendrometers were visited 6 times a year (January, February, March, June, September, and December) and the circumference change was measured with a caliper.

To measure needle growth, two branches were collected from 7 trees per plot every October (at the end of the needle growth period). The same trees were sampled for stem growth measurement. The branches were taken from 2 sides of the tree (east and west) at 6 m height.

2.4. Leaf gas exchange

From the 21 thinned plots, four neighboring plots (100, 200, 300, and unthinned control of 220 t ha^{-1}), sharing a NE aspect, were selected for seasonal gas exchange measurements. In each plot, five trees were selected according to the following criteria: (1) 19 < DBH < 25 cm; (2) 10 < Height < 14 m (one exception); (3) Healthy phenotype; and (4) Leaves accessible for measurement. In each tree, W and E facing sunlit, outer and lower canopy needle cohorts were marked for repeated measurement with an infra-red gas analyzer (Licor 6400, Licor, NE, USA). Leaf-scale conditions (photosynthetic active radiation, PAR, and vapor pressure deficit, VPD) and gas exchange rates (Net photosynthesis, A, and transpiration, T) were measured before (10:30–11:30) and after noontime (13:30–14:30) in three trees at each plot during eleven field days: 23 Jun 2010, 19 Jul 2010, 8 Dec 2010, 27 Feb 2011, 13 Apr 2011, 25 Jul 2011, 3 Nov 2011, 16 Feb 2012, 15 Mar 2012, 17 May 2012, and 21 Aug 2012. Raw data of leaf-scale measurements were subjected to analysis of variance (ANOVA), using JMP (Cary, NC, USA), to test the effects of stand density, date of measurement, time of day, and side of the canopy, on leaf-scale parameters: PAR, photosynthetically active radiation; VPD, vapor pressure deficit; A, assimilation rate; T, transpiration rate. Annual rainfall amounts in 2010, 2011, and 2012 were 289, 178, and 349 mm, respectively.

2.5. Upscaling from transient transpiration rates to diurnal water-use using diurnal T curves and tree allometric equation

To assess the interactions between leaf-scale response to thinning and the total water use of the tree at daily and ultimately seasonal time scales, we must scale short-term leaf-scale measurements. Measurements were taken routinely at two time-points during the day (~11:00 and ~14:00). Upscaling was performed using month-specific diurnal T curves constructed at the site based on leaf gas exchange measurements (Maseyk et al., 2008) and an allometric equation developed for this site from our previously published data on *Pinus halepensis* in Yatir (Gruenzweig et al., 2007). We developed a relationship between diurnal T and T measured at particular times during the day, as follows:

$$T_d = LA \cdot \frac{T_{d,m}}{T_{max,m}} \cdot \left(\frac{T_{11,m}}{T_{max,m}} + \frac{T_{14,m}}{T_{max,m}} \right) / 2 \tag{1}$$

where T_d is the diurnal water use amount; LA (m^2 tree^{-1}) is the average leaf area of trees at each density, estimated using measured DBH, height, and tree allometric equation developed at the site (Gruenzweig et al., 2007); $T_{d,m}$ is the monthly average of diurnal tree water-use amount (L day^{-1}); $T_{max,m}$, is the monthly average of maximum tree water-use amount (L h^{-1}); and $T_{11, m}$, and $T_{14, m}$ are the water-use rates at 11:00 and 14:00 for a month m. In this procedure,

Table 1
Summary of measurements taken during the study.

Parameter	Measurement frequency	Years	Method
Stem growth	6 times a year (Jan, Feb, Mar, Jun, Sep, Dec)	2010–2017	Manual band dendrometers on 7 trees at each plot
Needle length	Once a year (Oct)	2010–2017	The mean needle length of 1–3 year-old needles on 7 trees at each plot, at 6 m height from 2 different sides
Photosynthetically active radiation Assimilation Transpiration Vapour pressure deficit	5 times a year (Feb, Apr, Jul, Aug, Nov)	2010–2012	Needles from west and east sides of 5 trees at each plot. Measurements performed with the quantum yield sensor-equipped IRGA system

monthly specific diurnal T curves previously developed for the site (Maseyk et al., 2008) were normalized by the maximum T rate (T_{max}) for a specific day (representing a specific month). This allowed for testing how representative were the two point measurements. For example, in May, T rate at 11:00 and 14:00 were 85% and 70% of the diurnal maximum (occurring 9:00–9:30), termed $T_{11,m}/T_{max,m}$ and $T_{14,m}/T_{max,m}$, respectively. The diurnal T curves also showed that the diurnal water use (T_d) was proportional to T_{max}, with a ratio of 7.5–10, depending on the season, termed $T_{d,m}/T_{maxm}$. Applying the percentages above on each point measurement, allowed for the estimation of T_{max}, in turn used to estimate T_d. Last, leaf-scale values were multiplied by the average leaf area (LA) of trees at each density, estimated using measured DBH, height, and tree allometric equations. While we acknowledge that this approach is an approximation, we argue that estimates are sufficient to provide insight into relative magnitude and direction of leaf vs stand level changes in water flux across stand density (as discussed below).

2.6. Upscaling to local water yield

Tree-scale water use for the gas exchange measurement days in 2010–2012 was further converted to stand-scale water use by multiplying by the respective stand density. To scale from daily measurement to annual transpiration flux (T) at each density, mean monthly values were used. In cases where no monthly values were available, values were taken from the preceding or following month, depending on the annual water-use curve (Klein et al., 2014a). To test the hypothesis that thinning should proportionately increase the local water yield (WY, i.e. drainage below the rooting zone, possibly net recharge to groundwater), other hydrological components must be considered. In Yatir forest, surface runoff (R) and drainage from the rooting zone (D) are negligible (Shachnovich et al., 2008; Raz-Yaseef et al., 2010b) and the water table is below 300 m, eliminating the possibility of groundwater contributions (S) or other sources than precipitation (P) for evapotranspiration (ET). The long-term hydrological balance between the ecosystem water components (P = R + S + ET + D + WY) can therefore be simplified in Yatir to P ≈ ET + WY. The evapotranspiration flux is further partitioned into:

$$ET = T_t + E_s + I + T_u \qquad (2)$$

where T_t is tree transpiration, E_s is evaporation from soil, I is evaporation of water intercepted by plant foliage and T_u is transpiration from understory vegetation (usually confined to the rainy season). These four fluxes are ordered by their relative magnitude observed by previous monitoring in the Yatir forest water balance (Klein et al., 2014a), where the average stand density is 300 t ha^{-1}. The role of T_u was not measured in this study. Understory vegetation biomass at this site is assembled mostly of *Sarcopoterium spinosum*, and weigh less than 0.10 kg m^{-2} (Raz-Yaseef et al., 2010a, 2010b) and thus it is unlikely to contribute substantially to water and carbon fluxes. Evaporation from soil (E_s) was computed based on previously published relationships between Es and the percentage of tree cover in Yatir forest (Raz-Yaseef et al., 2010a, 2010b). I was computed from the difference between readings of rain gauges above and below the forest canopy (Raz-Yaseef et al., 2010a, 2010b).

2.7. Eco-hydrologic model

As an alternative, more process-based approach to upscaling, we also implement a coupled carbon-water cycling model for the site (RHESSys – Regional Hydro Ecologic Simulation System). RHESSys is a moderately complex ecohydrologic model that combines a carbon/nitrogen cycling model that is similar to many Dynamic Global Vegetation Models (DGVMs) and a spatially distributed hydrology model (Fatichi et al., 2016). RHESSys is selected here as moderate complexity approach that can capture key relationships between forest

density and moisture, radiation and carbon fluxes but is simple enough to generalize from short-term plots measurements to larger scales. RHESSys has been widely applied in forests under semi-arid and other climates to examine forest mortality (Tague et al., 2013), productivity (e.g. Tague et al., 2009; Vicente-Serrano et al., 2015), and water use and streamflow (Garcia and Tague, 2014; e.g. Bart et al., 2016). Linking field data with modeling in this study will support future work that expands to watersheds scales.

Details on RHESSys are provided in Tague and Band (2004), Tague et al. (2013), Garcia et al. (2016). RHESSys code is open-source and available online at https://github.com/RHESSys/RHESSys; (version 6.0 on the thinning code branch was used for this paper). Here we provide a brief overview of several key sub-models that are relevant to upscaling in this paper. RHESSys includes an hourly to daily time step model that explicitly simulates overstory and understory transpiration fluxes, canopy interception, and soil and litter evaporation losses. For both canopy moisture and carbon flux sub-models, the canopy is partitioned into sunlit and shaded components and, for this study, first year and older leaves. All evaporative fluxes are computed using a Penman or Penman-Monteith type approaches. A Jarvis-type sub-model of stomatal regulation is coupled with Penman-Monteith and includes vapor pressure deficit, soil water potential and other controls on stomatal conductance. The modelling accounts for diffuse and direct radiation and the attenuation of radiation, wind and moisture through the forest canopy as a function of overstory and then understory leaf area index. Water that reaches the forest surface is infiltrated into litter, shallow and ultimately deeper subsurface moisture stores. Soil parameters control the drainage rates, soil matrix bypass flow (or macropore flow) and soil matrix field capacity. Soil parameters for the site and ecophysiology parameters were based on values for loamy soil and pine from RHESSys parameter libraries, respectively, adjusted when possible based on site field observations (see Table S1 for a full list).

The carbon cycling model includes estimates of daily photosynthesis, respiration and the allocation of net primary productivity to growth is based on a combination of Farquhar photosynthesis, a Jarvis-type sub-model of stomatal regulation and age-resource dependent carbon allocation. Carbon allocation partitions net assimilation into leaf, root, stem and non-structural carbohydrate stores (Tague et al., 2013). Root depth and canopy height are parameterized functions of root and stem carbon stores respectively, using empirical parameters for Aleppo Pine (see Table S1 for parameters). Plant respiration increases with both air temperature and biomass following (Ryan, 1991). Leaf and fine root turnover are a fixed proportion of leaf and roots stores, using parameters derived from local measurements. Additional details on carbon cycling mechanisms and parameters can be found in Garcia et al. (2016). Although RHESSYs is commonly run at a hillslope to watershed scale to account for the lateral redistribution of moisture, here we implement the model for a single spatially homogenous stand. The model uses daily temperature and precipitation inputs to drive the simulation, adjusted when possible based on site field observations.

To initialize the model carbon and nitrogen stores, we simulated 40 years of spin-up to reach the approximate mean age of the Yatir stand. Meteorology forcing data included daily precipitation and daily maximum and minimum temperatures that were taken from the site flux tower (Grünzweig et al., 2003). For long-term spinup, meteorology forcing data was recycled (e.g. daily time series from 2000 was repeated). For thinning scenarios, meteorology data for actual time periods was used. Following spin-up, LAI, leaf, stem, and root carbon stores and canopy height as well as mean annual GPP and NPP estimates are similar to those reported by Maseyk et al. (2008) for the baseline, unthinned stand density (300 t ha^{-1}; Table S2). We include litter and grass understory, each with a ground cover of 75%. For simplicity, we show results only for baseline (300 t ha^{-1}) and intense thinning (100 t ha^{-1}). To compare with field measurements of post-thinning responses, simulations were run from 1 Oct 2009 (the beginning of the thinning treatment) to 30 Sep 2011. To simulate thinning, we removed

approximately 2/3 of forest carbon and nitrogen stores, and reduced tree density from $300\,t\,ha^{-1}$ to $100\,t\,ha^{-1}$. We then compared water and carbon flux estimates at both leaf and stand-scales for the high and low stand densities. Direct comparison of model estimates with observations is necessarily approximate since RHESSys estimates are averaged across sunlit and shaded leaves and aggregated to a daily time scale, while field measurements are instantaneous measurements for single leaves. Further, leaf-scale gas exchange measurements reflected a sample of 11 campaign days within the simulation period, while the model estimated daily fluxes throughout the year. Nonetheless, we investigated whether the general patterns found in the field data were consistent with model results. Finally, to assess how the changes in water and carbon fluxes may vary with meteorological forcing conditions (temperature, precipitation and vapor pressure deficit), additional simulations computed leaf and stand-scale flux estimate for all hydrological years between 2002 and 2007. Within this timeframe, annual precipitation ranged from 224 mm to 373 mm.

3. Results

3.1. The effect of stand density on leaf-scale conditions, gas exchange rates, and tree growth

Average leaf-scale gas exchange measurements from 11 field days along two years (2010–2012, with average annual precipitation of 236 mm) showed variable stand density effects (Fig. 2). The average
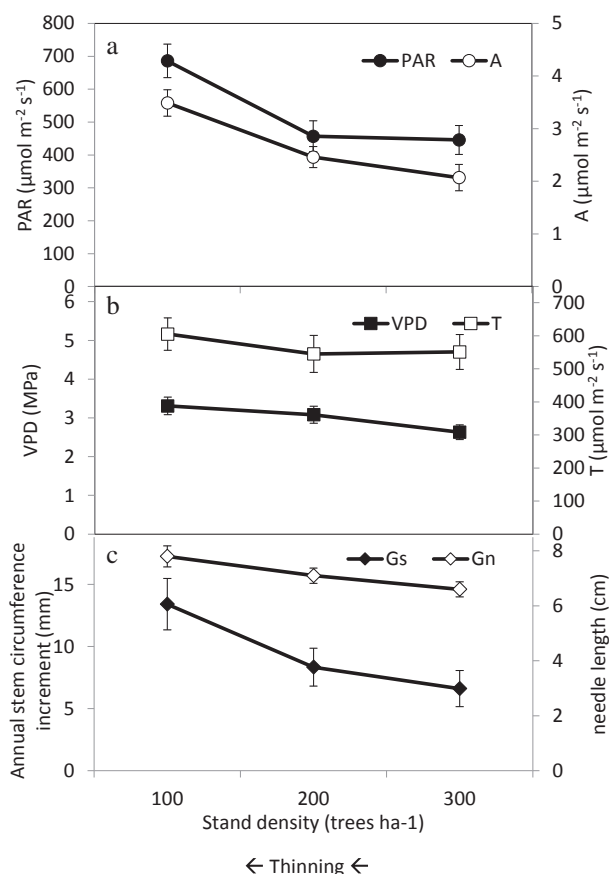

Fig. 2. Stand-density influence on leaf-scale photosynthetically active radiation (PAR) and net assimilation (A), (a); on vapor pressure deficit (VPD) and leaf transpiration (T), (b); and on stem growth (Gs) and needle length (Gn; c) in Yatir forest. Each data-point at top and middle panels is the mean (± SE) of 120 observations in 10 field days (2010–2012). Stem growth and needle length data-points are means (± SE) of 252 and 84 observations, respectively, in 36 field days (2010–2016).

Table 2
ANOVA Table for the effects of stand density, date of measurement, time of day, and side of the canopy on leaf-scale parameters: PAR, photosynthetically active radiation; VPD, vapor pressure deficit; A, assimilation rate; T, transpiration rate. Asterisks denote the effects at significance level of $0.05 > \alpha > 0.01$ (*) and of $\alpha < 0.005$ (**).

Response	Factor	t ratio	P > t
PAR	Stand density	−3.93	0.0001**
	Date	−1.17	0.2439
	Time (morning/afternoon)	0.10	0.9226
	Side (East/West)	2.47	0.0141*
VPD	Stand density	−2.11	0.0357*
	Date	−1.41	0.1592
	Time (morning/afternoon)	2.69	0.0074**
	Side (East/West)	0.92	0.3589
A	Stand density	−4.49	< 0.0001**
	Date	−1.84	0.0663
	Time (morning/afternoon)	−2.93	0.0036**
	Side (East/West)	1.51	0.1322
T	Stand density	−1.11	0.2682
	Date	2.61	0.0095**
	Time (morning/afternoon)	−2.44	0.0151*
	Side (East/West)	1.13	0.2592

photosynthetically active radiation (PAR) at the surface of the measured leaves was > 50% higher at the low density stand than at the other densities. Inter-tree shading on the lower branches, where measurements took place, limited PAR to ~$450\,\mu mol\,m^{-2}\,s^{-1}$ in both 200 and $300\,t\,ha^{-1}$. Net photosynthesis (A) followed the changes in PAR and decreased from 3.5 to 2.5 and $2.1\,\mu mol\,m^{-2}\,s^{-1}$ in 100, 200 and $300\,t\,ha^{-1}$, respectively. Differences in vapor pressure deficit near the leaf surface (VPD) across densities were milder and not significant, suggesting a high level of eddy mixing within the canopy. Similarly, average transpiration rates (T) were only 10% higher for the low density stand relative to higher densities, but this difference was not statistically significant. The decrease in A and the minor decrease in T with increasing density suggest that the low density stand had higher tree-scale water-use efficiency (WUE). Stand density was significantly affecting three of the four leaf-scale parameters, i.e. PAR, VPD, and A (Table 2). Other factors (date, time of day and side of canopy), also influenced some of these parameters, but to lower extent. PAR was sensitive to the side of the canopy being measured, with significantly higher light in East vs. West side. VPD and A were sensitive to the time of the measurement, with significantly higher VPD in the afternoon and higher A in the morning; and T was sensitive to the date of measurement, with significantly higher T in wet season days. Stand density effects varied with season whereby the thinning-induced enhancement of A and T tended to decrease in late summer and winter relative to spring (March–May) (Fig. S3). Annual basal area increment and needle length decreased as stand density increased (Fig. 2c; Fig. S4). The difference between basal area increment for the lowest density and the highest density was statistically significant (P-value = 0.034). Density effects on needle length were milder, without significant difference between the densities.

3.2. Upscaling to stand-scale gas exchange rates using leaf area index (LAI)

Gas exchange rates, measured per leaf area, were up-scaled to stand-scale values (rates per ground area) using concurrent LAI data. This empirical approach ignores the effects of canopy architecture, gradients within the canopy, or thinning stress. By the end of the first year following the thinning (2010), LAI values were 0.90, 1.33 and 1.54 in 100, 200 and $300\,t\,ha^{-1}$, respectively. This suggested that differences in stand architecture were higher between 200 and $100\,t\,ha^{-1}$, than between 300 and $200\,t\,ha^{-1}$, in agreement with the differences in PAR (Fig. 2a). Multiplying T and A averages in Fig. 2 by these LAI values
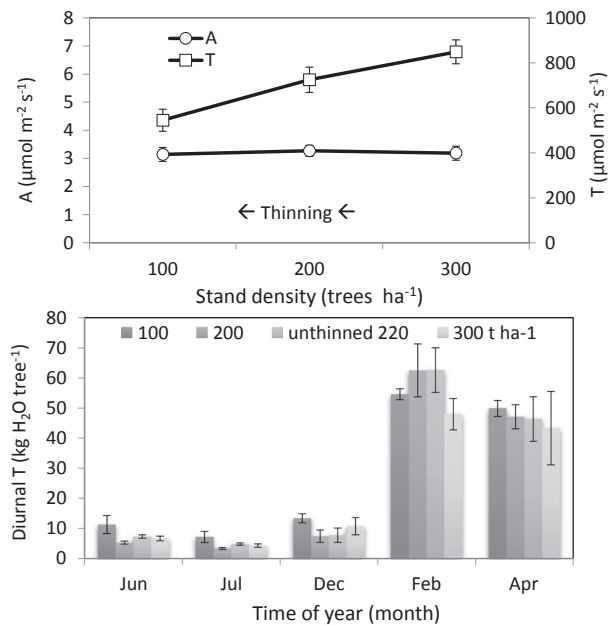
Fig. 3. Stand-density influence on stand-scale T and A (a) in Yatir forest. Each data-point is the mean (± SE) of 120 observations in 10 field days over two years. Effects of changes in stand density on tree-scale transpiration in five field days in 2010 in Yatir forest (b). Each bar is the up-scale mean (± SE) of 12 observations.

yielded a preliminary estimate of stand-scale gas exchange rate (Fig. 3a). The thinning significantly decreased T, from 0.85 to 0.72 and 0.55 mmol m^{-2} s^{-1} in 300, 200 and 100 t ha^{-1}, respectively, but maintained A at ~3.2 µmol m^{-2} s^{-1}. The decline in stand-scale T with reduced density reflect the impact of canopy reduction while the similar A across densities reflects the greater leaf-scale A with thinning.

3.3. The thinning bias

The stand density reduction obtained by the abrupt, mechanical, thinning, cannot simulate differences in native stand densities, where relationships between individual trees (e.g. crowns competing for light, root systems competing for soil moisture, etc.) are often in equilibrium. We examined the impact of this effect by including an unthinned control stand, at a native stand density of 220 t ha^{-1}. Using the average leaf-scale gas exchange rates in 300 and 200 t ha^{-1} (Fig. 2), the linearly interpolated A and T rates in 220 t ha^{-1} are estimated at 2.4 µmol m^{-2} s^{-1} and 0.55 mmol m^{-2} s^{-1}, respectively. The measured leaf-scale A and T averages in the native 220 t ha^{-1} stand were 3.1 µmol m^{-2} s^{-1} and 0.63 mmol m^{-2} s^{-1}, respectively (data not shown). Thus, trees at the thinned stands were less active than trees at the control stand of similar density, suggesting the possibility of thinning stress.

3.4. Upscaling to stand-scale gas exchange rates using empiric relationships

Using our upscaling approach (see Methods), estimates of diurnal, tree-scale, transpiration were produced for each density and field day in 2010 (Fig. 3b). In Yatir and other semi-arid forests, tree water use and other activities are largely governed by the sharp seasonality in precipitation. This creates a large contrast between the dry season (summer and autumn) and the wet season (winter and spring). In 2010, individual tree water use was estimated at 4–13 kg d^{-1} in the dry season and 43–63 kg d^{-1} in the wet season (Fig. 3b), in agreement with concurrent sap flow measurements at 300 t ha^{-1} in this site (not shown). Differences between the densities were small and mostly not significant. In the dry season (June–December) tree water-use was 65%
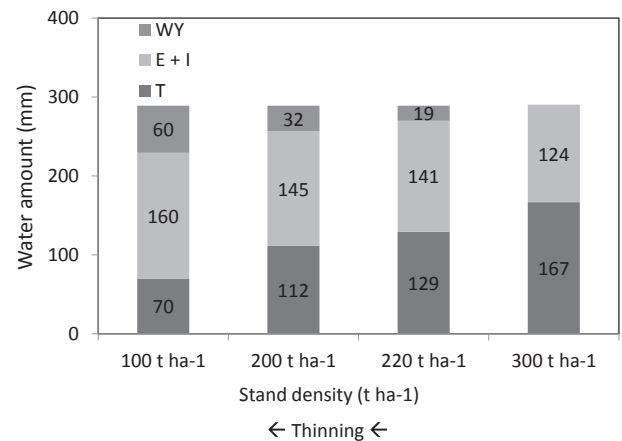

Fig. 4. Effects of changes in stand density on tree-scale water use in five field days in 2010 in Yatir forest. Each data-point is the up-scale mean (± SE) of 12 observations.

higher at 100 t ha^{-1} relative to water-use at other densities. However, differences at the annual time scale were not significant.

3.5. The effect of stand density in a semi-arid pine forest on the local water yield

Estimates of diurnal tree-scale water-use were further up-scaled to annual stand-scale estimates (Fig. 4). Stand-scale transpiration scaled with density, from 70 to 112 and 167 mm yr^{-1} in 100, 200 and 300 t ha^{-1}, respectively. This increase was proportional to the increase in the number of trees per area for the moderate thinning (e.g. 300/200 = 167/112), but less than proportional for the heavy thinning (e.g. 300/100 > 167/70). The estimate of annual T in 100 t ha^{-1} (70 mm) was higher than the expected amount (56 mm), due to the observed mild decrease in leaf-scale T with increasing density (Fig. 2b). There was a considerable decrease in the sum of E_s and I, from 160 to 145 and 124 mm in 100, 200 and 300 t ha^{-1} (Fig. 4). The residual water amount, or water yield, WY, reflects the tradeoff between T and E_s + I. The increase in T_t was mildly higher than the decrease in E_s + I, yielding WY amounts of 60, 32 and 0 mm in 100, 200 and 300 t ha^{-1}. These small amounts indicated that the hypothesis that thinning should proportionally increase WY was not confirmed in this semi-arid ecosystem.

3.6. Estimating stand density effects on leaf- and stand-scale gas exchange rates using an eco-hydrologic model

Similar to field measurements, RHESSys estimates show an increase in leaf-scale absorbed PAR with thinning. Increases varied over the year, with greatest increases in May (mean 44% increase; Table 3 and Fig. 5a). Model estimates and field measurements of leaf assimilation (A) and transpiration (T) agreed relatively well, with most measurements falling within the range of modelled estimates (Fig. 5b, c). Both model and measurement showed a higher A and a similar T with thinning, and captured the seasonal trends, more so in the model output. There was a thinning-induced increase in leaf-scale A, although the modeled average increases were substantially lower than the increase measured in the field: the modeled mean increase was 20%, while the observed increase was 68%. We note, however, that the model estimates showed substantial daily and seasonal variation in assimilation rates, ranging from 0 to 10 g C m^{-2} day^{-1} (Fig. 5b), and substantial daily variation in the thinning-induced increase in leaf-scale assimilation, from 0 to 2 g C m^{-2} day^{-1} for 100 vs. 300 t ha^{-1}. RHESSys estimated a small, but significant, 15% increase in leaf-scale T associated with thinning (Table 3); similar to the 10% increase from

Table 3

The effect of thinning on stand and leaf-scale carbon and water fluxes calculated by the eco-hydrologic model RHESSys for Yatir semi-arid pine forest. Leaf-scale values are averaged over day and season. LAI, leaf area index; NPP, net primary productivity; PAR, photosynthetically active radiation.

Parameter	300 trees ha^{-1}	100 trees ha^{-1}	Percent difference with thinning
Stand-scale transpiration (mm year^{-1})	149	78	−47
Stand-scale evaporation (mm year^{-1})	144	208	+44
Total water flux (mm year^{-1})	293	287	−2
Stand LAI	1.47	0.5	−66
Stand-scale assimilation (g C m^{-2} year^{-1})	520	318	−38
Stand-scale NPP (g C m^{-2} year^{-1})	241	155	−35
Leaf-scale PAR (μmol m^{-2} s^{-1})	126	226	+18
Leaf-scale assimilation (μmol m^{-2} s^{-1})	2.3	2.75	+19
Leaf-scale transpiration (mm day^{-1})	0.64	0.56	+14

observed estimates. As with A, RHESSys estimates of daily leaf-scale T varied substantially within and between seasons. The change in leaf-scale T in the thinned stand relative to baseline ranged from −0.6 to 0.8 mm m^{-2} day^{-1} (Fig. 5c). RHESSys estimated higher T from thinned stands particularly during May and June, reflecting a modelled decrease in late season water stress for the thinned stand. Noteworthy, RHESSys assumes that trees in the thinned stand have access to any surplus rooting zone water that is released by the removal of neighboring trees.
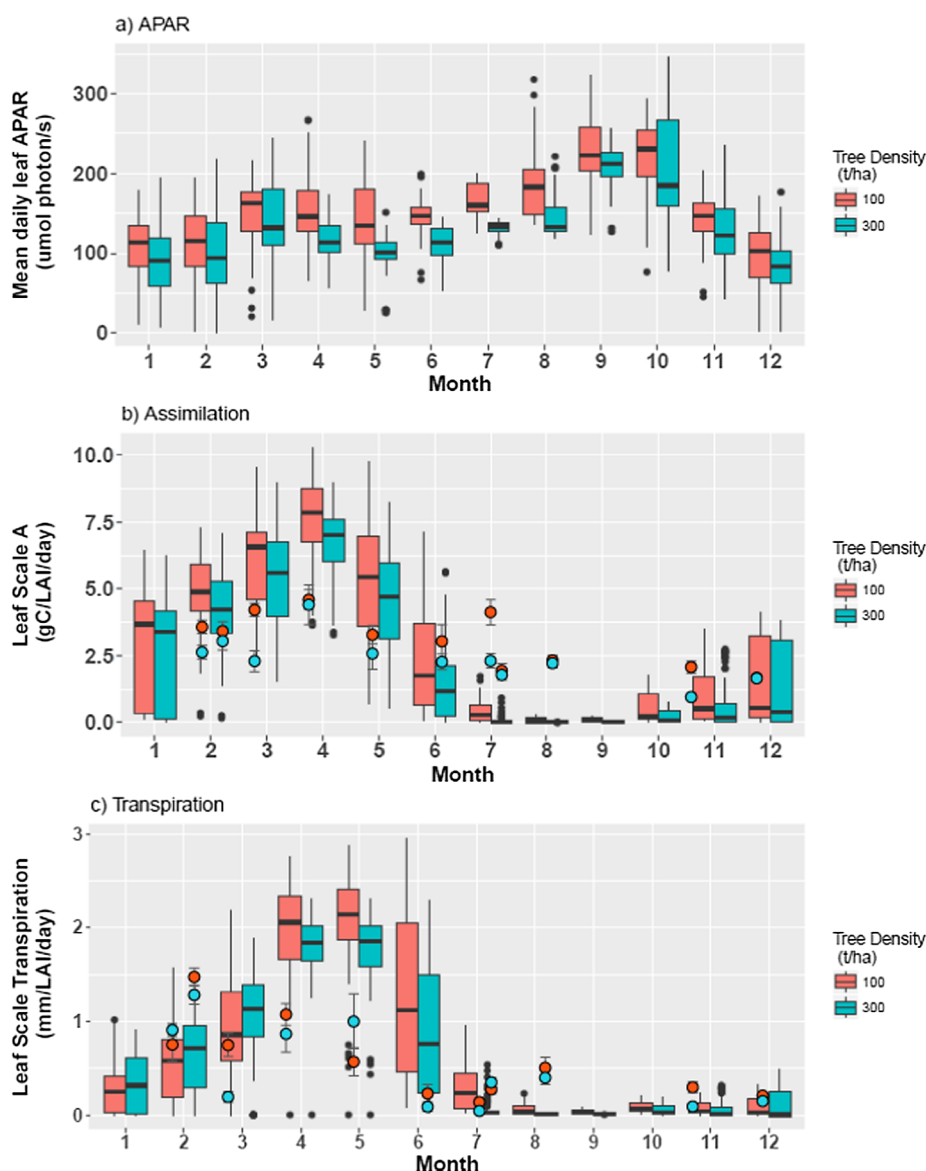

Fig. 5. RHESSys model outputs for monthly dynamics of leaf-scale absorbed photosynthetically active radiation (a), carbon assimilation (b), and transpiration (c). Box-plots show daily variation in each month for hydrological years 2010–2011 for both 100 trees ha^{-1} and 300 trees ha^{-1} stands. Data points in (a) and (b) are means based on the needle gas exchange measurements in the field. Each data-point is a mean ± standard error of East and West side measurements of three trees in morning and afternoon hours (*n* = 12).
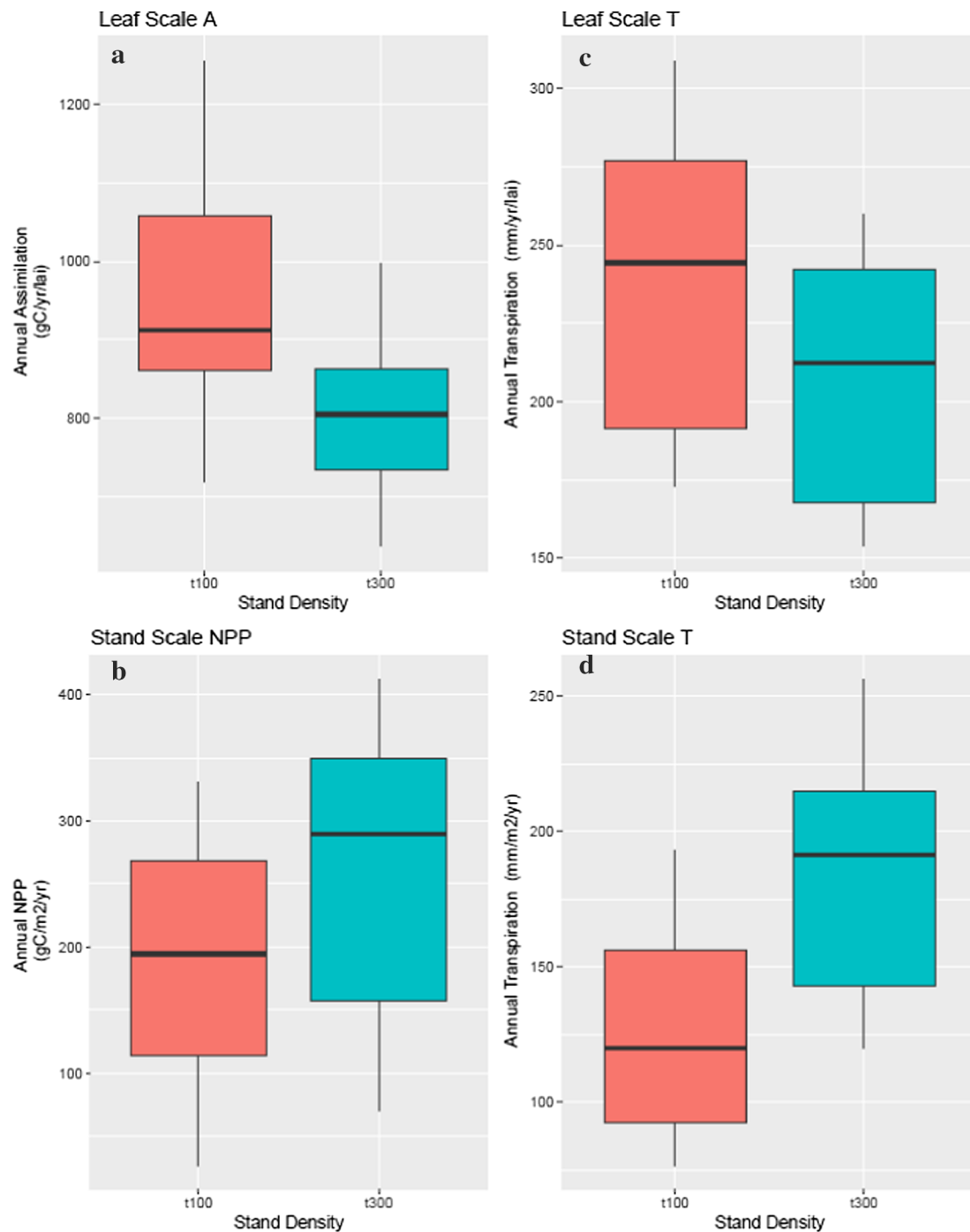
Fig. 6. RHESSys estimates of annual leaf-scale (a, c) and stand-scale (b, d) fluxes of carbon (a, b) and water (c, d). Box-plots show inter-annual variation for the hydrological years 2002–2007 for both 100 trees ha^{-1} and 300 trees ha^{-1} stands in the semi-arid pine forest at Yatir.

In other words, we assumed that root area expands to capture available water. This may be an overly simplistic assumption and additional research will be designed to investigate how root water access changes following thinning and incorporate this dynamics into the model.

At the stand and annual spatial and temporal scales, RHESSys estimated a moderate decline in NPP and a greater decline in stand-scale transpiration with thinning (~35% and 50% declines respectively; Table 3). RHESSys estimates of annual stand-scale water partitioning were similar to those estimated with the empirical scaling approach. Both approaches showed a substantial thinning-induced increase in evaporation (from soil evaporation), and suggested that these evaporation increases generally compensated for losses in transpiration

with thinning, resulting in negligible changes to WY (< 5%). When we repeated our analysis for different meteorological forcing conditions, the general pattern of differences between 100 t ha^{-1} and 300 t ha^{-1} stands were similar to those reported for 2010–2011. At the leaf-scale, assimilation and transpiration both increased for the thinned forest, but relative increases in assimilation were greater and more consistent across years relative to leaf-scale transpiration increases (Fig. 6). Greater leaf-scale assimilation in the 100 t ha^{-1} did not fully compensate for the loss of leaf area with thinning but it did lead to greater percentage declines in stand-scale transpiration relative to assimilation (Fig. 6). As with 2010–2011 hydrological year, losses in transpiration in the 100 t ha^{-1} stand were balanced by increased evaporation.
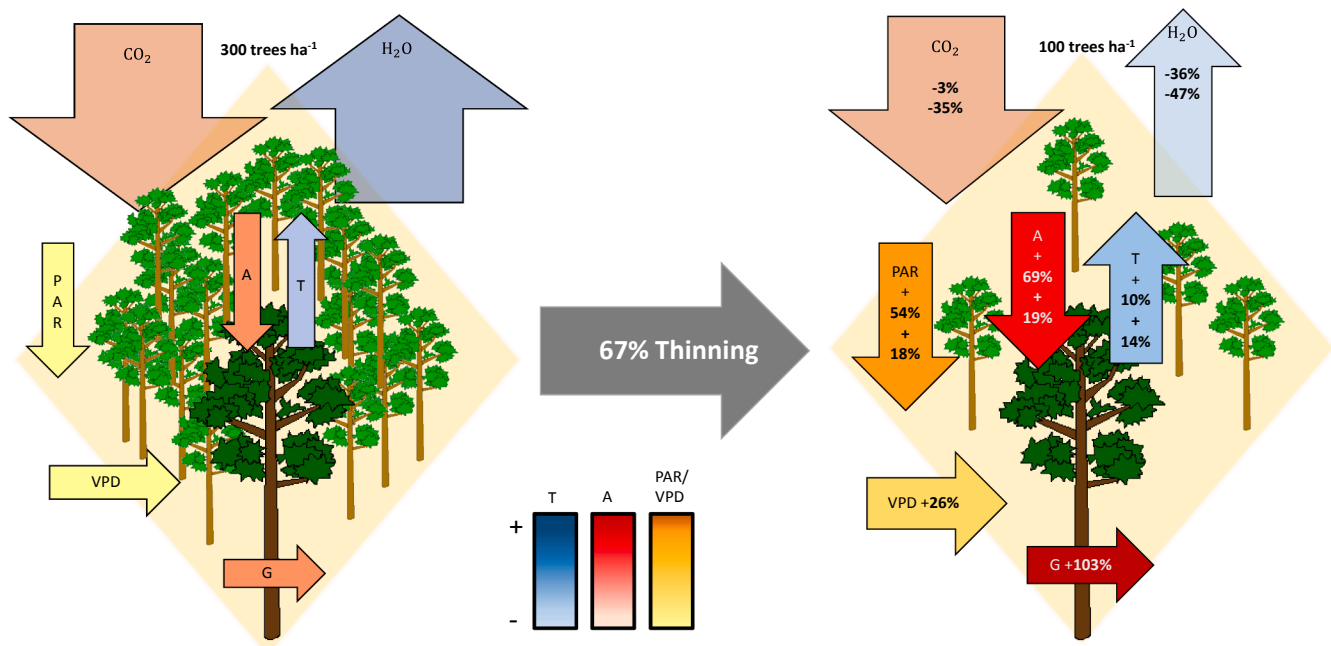
Fig. 7. Summary of the observed and modelled changes of forest thinning on major tree and stand water, carbon, and energy fluxes. Arrow direction denotes flux direction; arrow size and color intensity denotes flux magnitude. Values on top are measured and up-scaled from leaf-scale measurements; values in the bottom are modelled by RHESSys. The decrease in stand density increased the photosynthetically active radiation (PAR) below the canopy and, less so, the vapor pressure deficit (VPD). As a result, tree-scale carbon assimilation (A) and growth (G) increased considerably, while transpiration (T) increased mildly. This tree-scale intensification compensated for the thinning-involved tree loss, while reducing stand-scale water-use.

4. Discussion

Our long-term thinning experiment in a semi-arid pine forest quantified the major effects on carbon and water fluxes (Fig. 7), partially confirming our hypothesis, while bringing additional insight. We observed the expected increase in below canopy PAR, and a milder increase in VPD. For remaining trees, tree-scale carbon assimilation (A), transpiration (T), and growth (G) also increased, albeit the increase in A being higher than expected. This thinning-induced photosynthetic enhancement relates to the higher light penetration. The conclusion that light is a limiting factor in our light-abundant, water-poor, semi-arid forest is counter-intuitive. However, while the expected soil moisture limitation does control summer fluxes, most of the tree activity in Yatir occurs during the winter when soil water availability is generally high and radiation is lower (Maseyk et al., 2008; Rotenberg and Yakir, 2010). Increased growth, stimulated by thinning, also produces new needles that have higher water use efficiency, further enhancing photosynthesis. Remaining trees, which also benefitted from increased water availability, were able to translate it into higher activity and growth at the tree scale. On the other hand, at the stand-scale, these tree scale increases in A and T are only partially compensated for by the net loss of trees. Therefore, in the first two years following thinning, stand level CO_2 uptake and water-use were similar or lower compared to the unthinned state.

4.1. Stand density effects on transpiration

For measured data, there were mild, non-significant changes in tree-scale transpiration (Fig. 3b). Deviations from a linear response in leaf-scale T (Fig. 2b) carried over to higher scales and stand-scale T was not always proportional to density, in agreement with an earlier study, showing that T increases by 32% when canopy cover doubles (Moreno and Cubera, 2008). This observation is also in agreement with Bréda et al. (1995), who found in an oak forest that differences in stomatal conductance (g_s) between density treatments appeared only during a water shortage, and affected mainly the closed stand. Conversely,

studies in Spain showed a different trend, where leaf T and g_s decrease as density increases (Moreno-Gutiérrez et al., 2011; Del Campo et al., 2014). The difference between our results and those of Moreno-Gutiérrez et al. (2011) could be a result of the higher stand densities in the latter (1000 thinned to 770 and 550 t ha^{-1}). At the stand-scale, we observed an increase in T with density increment, corresponding to Forrester et al. (2012). On the other hand, Del Campo et al. (2014) showed that transpiration at the stand-scale was similar across densities. The contradiction might relate to the difference in climate between the sites: in the Spanish study the mean annual precipitation during the measurements was 772 mm, while in our site it was 236 mm. Differences in subsurface water storage characteristics may also be an important control on transpiration responses to changing density (Phillips et al., 2016) and we note that previous research in the Yatir forest demonstrate that the presence of high water holding capacity above a deeper clay confining layer results in a particularly high plant accessible subsurface water storage (Klein et al., 2014a). Interestingly, although trees growing in our thinned plots had lower competition on water than in the control plots, the high VPD meant that trees might have been unable to use this excess water due to hydraulic constraints. The xylem of *P. halepensis* is relatively sensitive to drought due to embolism (Klein et al., 2011, 2016) and therefore g_s and T are low at high VPD. In fact, VPD in the thinned plots was mildly higher than in the unthinned plots (following the higher PAR; Fig. 2a). We also note however that additional tree-scale transpiration due to reduced competition is most likely to occur at the end of the wet season when additional water remains. It may be that this period of time was under-sampled in our experimental design. Indeed, RHESSys model results do show additional transpiration from thinned trees during that period. It is possible that leaf-scale T could be enhanced with thinning in a more humid area or in a more drought-resistant tree species.

4.2. Stand density effects on assimilation and water-use efficiency

In our study, photosynthesis decreased with forest density: the lowest density showed the highest photosynthesis rate (Fig. 2a). This

expected finding confirms earlier observations in Mediterranean pine forests (Moreno and Cubera, 2008; Moreno-Gutiérrez et al., 2011). At the stand-scale we reported comparable levels of carbon uptake (Figs. 3 and 6), suggesting a limited impact of thinning on carbon sequestration. This unchanged carbon uptake, combined with the reduced transpiration, means higher water-use efficiency (WUE) following thinning at the stand-scale. Thinning-induced WUE increase was reported in multiple studies (Forrester et al., 2012; Fernandes et al., 2016; Navarro-Cerrillo et al., 2016; but see Moreno-Gutiérrez et al., 2011). As mentioned, stand densities in the latter study were higher than here, further highlighting the complexity in interpreting data from such experiments.

4.3. Stand density effects on tree growth

Thinning was previously shown as inducing higher stem growth (Moreno-Gutiérrez et al., 2011; Delas Heras et al., 2013; Olivar et al., 2014; Ruano et al., 2013; Del Campo et al., 2014; Calev et al., 2016; Navarro-Cerrillo et al., 2016). Stem growth rate under thinning is a function of tree species, age, size, the time since thinning and the removed and remaining competition (Kariuki, 2008). Additionally, short-term effects can be very different, and even opposite at the longer term. There is a debate if time that passes since thinning is associated with a decrease in growth, as shown in *Eucalyptus sieberi* (Kariuki, 2008) or with increase in growth until several years after thinning. For example, Ruano et al. (2013) observed an increase in growth until the 5th year after thinning, and Navarro-Cerrillo et al. (2016) observed the highest growth enhancement after 9 years in *P. pinaster, P. sylvestris* and *A. pinsapo* in thinned plots. In our study, we observed the highest growth enhancements after 5 and 7 years (Fig. S4), in correlation with the higher precipitation in these years (320–352 mm). At high precipitation, growth increases respectively (Bréda et al., 1995; Moreno-Gutiérrez et al., 2011; Olivar et al., 2014). Overall, in our study, annual precipitation influenced growth rates more than the time after thinning. The mean growth enhancement was 103%, which seems a major effect. But how does this rate compare with similar effects at other sites? We summarized observations from other forest thinning studies conducted on *P. halepensis* and from studies discussed here (Table 4). Next, thinning-induced growth enhancement was plotted against the thinning intensity (Fig. 8). The resulting correlation was best described by an
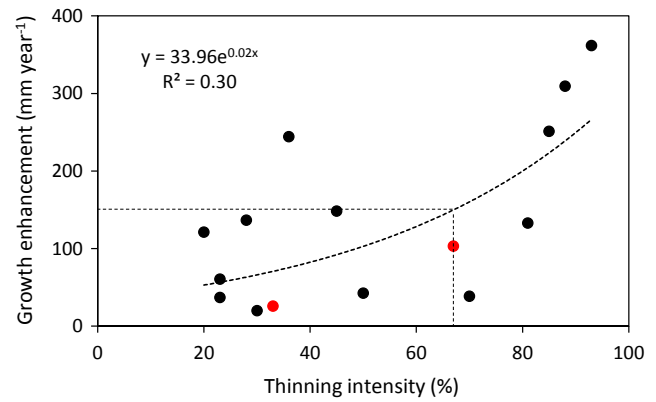
Fig. 8. Thinning-induced stem growth enhancement as function of thinning intensity, based on the results in this study (red) and other studies (black), as detailed in Table 2. Dashed lines mark the expected growth enhancement (y-axis) for the higher thinning intensity in our study (x-axis). (For interpretation of the references to color in this figure legend, the reader is referred to the web version of this article.)

exponential relationship, whereby high growth enhancements are expected at high thinning intensities (Fig. 8). According to the combination of all studies and at our thinning intensity, the expected growth enhancement was ~150%. It is possible that the water limitation in our study site, which was more acute compared to other sites, can explain the observed lesser enhancement. Essentially, the lack of available water prevented trees in the thinned plots to maximize their new growth potential, despite the decrease in competition. The highest growth enhancement was observed in a study at a temperate forest (Kariuki, 2008), and the second highest in a study which had unexpectedly higher precipitation (Del Campo et al., 2014), supporting our hypothesis.

4.4. Influence of thinning on water yield

The critical role that forests play in the hydrological cycle has raised some concerns about their negative impact on WY, with evidence that

Table 4
The effect of thinning on stem growth (circumference) in this study and in studies reported in the scientific literature. To facilitate comparison, growth was converted from diameter or basal area increment to circumference where needed. Climate types: Mediterranean (Md), Semi-arid (SA), and Temperate (Tm). Tree species: *Quercus petraea (Qc), Pinus halepensis (Ph), Pinus pinaster (Pp), Pinus sylvestris (Ps), Abies pinsapo (Ap), Pinus nigra (Pn), Eucalyptus sieberi (Es), Eucalyptus consideniana (Ec), Eucalyptus radiate (Er)*, and *Eucalyptus baxteri (Eb)*.

Stand density (tree ha^{-1})	Thinning intensity (%)	Stem growth (control, mm year^{-1})	Stem growth (thinned, mm year^{-1})	Thinning-related growth enhancement (%)	Climate	Species	Study year	Thinning year	Reference
3998 > 3077	23	5.55	7.6	36.94	Tm	*Qp*	1992–1993	1992	Bréda et al. (1995)
1760 > 1232 > 528	70	9.36	12.96	38.51	Md	*Pp, Ps, Ap*	1990–2005	1989	Navarro-Cerrillo et al. (2016)
	30	9.36	11.21	19.82					
300 > 200 > 100	67	6.6	13.4	103.03	SA	*Ph*	2010–2017	2009	**This study**
	33	6.6	8.3	25.76					
2000 > 1600	20	3.98	8.8	121.11	Md	*Ph*	2009	2004–2007	Ruano et al. (2013)
1600 > 1150 > 1020	36	2.142	7.38	244.35	SA	*Pn*	1993–2007	1993	Martín-Benito et al. (2010)
	28	2.142	5.07	136.69					
1489 > 744 > 478 > 178	88	4.08	16.71	309.56	SA	*Ph*	2009–2011	2008	Del Campo et al. (2014)
	67.8	4.08	39.61	870.83					
	50	4.08	5.82	42.65					
971 > 537 > 245	93	5.75	26.55	361.74	Tm	*Es, Ec, Er, Eb*	1968–2007	1968	Kariuki (2008)
	85	5.75	20.19	251.15					
	81	5.75	13.389	132.86					
1000 > 770 > 550	45	0.66	1.64	148.48	SA	*Ph*	2005–2009	2004	Moreno-Gutiérrez et al. (2011)
	23	0.71	1.14	60.56					

afforestation reduced downstream water availability (Farley et al., 2005; Jackson et al., 2005). Our results, on the contrary, show that leaf-to stand-scale feedbacks of stand density on transpiration and evaporation mean little effect of forest cover on WY. Recent studies provided several explanations to observations of low impact of forests on WY. Firstly, Ellison et al. (2012) proposed that trees can reduce runoff at the small catchment scale, whereas at larger scales, trees are more clearly linked to increased precipitation and water availability. This explanation can be ruled out in the case of a relatively small forest like Yatir. Secondly, a trade-off between tree and understory transpiration (T_t and T_u, respectively) was claimed to explain increased stream-flow in semi-arid basins following an increase in stand density (Guardiola-Claramonte et al., 2011). Such explanation cannot suffice for Yatir forest, where T_u is usually limited to the wet season and also controlled by grazing. In addition, differences in the intensity of herbaceous vegetation among our density stands were not significant. But it is the partitioning between E and T that can explain the low impact of forests on WY. Wang et al. (2010) showed an increase in fractional contribution of T to ET as woody cover increased, from T/ET = 0.61 at 25% woody cover to T/ET = 0.83 at 100% cover. For comparison, T/ET ratios calculated from Fig. 4 are 0.24, 0.39 and 0.58 in 100, 200 and 300 t ha^{-1}, respectively. As shown here, the tradeoff between T and E_s is critical especially in semi-arid ecosystems, where surface runoff and groundwater recharge are minor hydrological components, and E_s is a major player (Simonin et al., 2007; Raz-Yaseef et al., 2010a, 2010b). In a forest located in the dry timberline, this tradeoff controls the water balance at the entire range from zero to full vegetation cover with little effect on WY (Merzer, 2007).

4.5. Stand density effects using model simulations

Consistent with field observations, RHESSys estimates showed that while thinning reduces both transpiration and assimilation, the reduction in assimilation was lower (Table 3). Peak season model estimates were higher than measurements (Fig. 5b, c), but these were done mostly during drier conditions than average (annual precipitation in 2011 was just 178 mm). Model estimates also support conclusions from field observations that losses in transpiration with thinning are largely compensated for by increases in surface evaporation fluxes rather than increases in groundwater recharge. RHESSys estimates further suggest that these patterns are likely to be robust across recent year-to-year variation in climate (Fig. 6d). RHESSys estimates also similarly show that stand-scale productivity (NPP) declines with thinning were lower than the declines in stand-scale transpiration. The modelling study offers two explanations that complement observation based analysis (1) RHESSys, estimates a leaf-scale enhancement of assimilation with thinning, similar to observations, and (2) RHESSys estimates a reduction in stand-scale respiration with thinning. In RHESSys, both transpiration and assimilation increase with PAR, with slightly greater assimilation increases. In general, conditions of light saturation result in a hyperbolic relationship between PAR and assimilation, whereas transpiration may continue to increase at higher PAR (Baldocchi and Amthor, 2001). Under these conditions we might expect lower water-use efficiency in the thinned (higher leaf-scale PAR) forest. However, the photosynthetic efficiency also varies with needle age and differs for sunlit and shaded leaves (Fig. S5). One explanation for this is the greater proportion of both sunlit and new (first year of growth) needles in thinned trees (Table S3). Following an approach similar to Porté and Loustau (1998), RHESSys accounts for greater photosynthetic efficiency of young and sunlit needles by varying photosynthetic parameters (fraction of nitrogen in rubisco and quantum efficiency; Table S1). Direct measurement of water-use efficiency for needles of different ages and sunlit/shaded canopy positions for Aleppo pine confirms that younger and sunlit needles have greater water-use efficiency (Fig. S5; also Maseyk et al., 2008). These changes in leaf physiology, and associated parameters in RHESSys, offer an explanation for estimated

increase in water-use efficiency in the thinned stand. Total stand-scale respiration losses from plant organs, including roots, also contribute to smaller declines in NPP (relative to transpiration) with thinning. The impact of increased water use due to a greater proportion of younger and sunlit leaves may be short-lived. This study focused mostly on the first two post-thinning years. Further, how PAR, VPD and other microclimate and plant physiological parameters influence water-use efficiency is rather complex, and thus these findings may vary with species, thinning density and microclimate conditions (Shi et al., 2014).

A key question is whether remaining trees, following thinning, have access to remaining water. RHESSys model assumes that roots share water. Field based observations were not frequent enough to test the extent of additional water access, particularly given the expected intra-seasonal variation in assimilation. A recent review (Phillips et al., 2016) similarly highlights the importance of improving the ability to model the extent to which individual tree root systems overlap and how root growth change with conditions, including thinning. However, field measurements do confirm increased productivity (greater needle growth per tree) in the thinned forests. If roots do overlap, and remaining trees have access to additional water following thinning, there are some interesting implications of extending the period of higher assimilation rates later into the season. For example, water-use efficiency typically decreases with higher VPD (Ponton et al., 2006) so we might expect lower water-use efficiency in the thinned forest if more of the assimilation occurs during the high VPD summer period. However, other competing mechanisms noted above may balance this reduction in WUE at aggregate seasonal to annual time scales. Regardless of changes in water-use efficiency, both model and observations point to increases in evaporation following thinning and suggest that gains in water yield are likely to be small. This result is consistent with other studies in Mediterranean forests that have found little or no change in total ET or streamflow with small changes in forest density (e.g. Simonin et al., 2007; Biederman et al., 2014).

4.6. Synthesis and implications

Our study at the dry timberline showed that thinning decreased carbon assimilation, but less than expected given the decrease in LAI. Thinning increased leaf-scale PAR, the ratio of sunlit to shaded needles, and the ratio of new to old needles; the combination of the above leading to greater leaf-scale assimilation. The forest water balance did not change, because the decreases in transpiration were compensated for by increases in evaporation and by phenological changes (trees in thinned stands maintained transpiration longer into the dry season). From an eco-physiological perspective, our results highlight the fact that light availability can act as a limiting factor even in a light-abundant forest.

Together with the expected benefits to forest sustainability (major) and WY (minor), thinning to 200 t ha^{-1} might be recommended for forest management in Yatir. Such recommendation should be taken with precaution due to the observed, yet unresolved effects of thinning stress, as previously described (Peltola et al., 2002; Pukkala et al., 2002; Di Matteo et al., 2010; Kariuki, 2008). Thinned stands are more resistant to drought stress and recover faster than unthinned stands (Moreno-Gutiérrez et al., 2011; Sohn et al., 2013). Indeed, following the drought of 2011, we measured the highest stem increment at 100 t ha^{-1} plots. Such increments were not significant in the other plots. Tree-to-tree competition is lacking in our analysis and will need careful parameterization. Competition level should affect forest sustainability, which is a major concern in forests under climate change. Moreno and Cubera (2008) found that the increase in tree-to-tree competition with stand density was much more significant at dry sites. In those sites, tree thinning is recommended as a way to maintain tree functioning. It can be argued that drought-induced tree mortality is a form of self-thinning. On the other hand, drought can lead to entire stand losses (tragedy of the commons scenario); and tree mortality typically increases the risk to

surviving trees via biotic infestations. Prescribed thinning can avoid these problems, while still maintaining forest carbon sequestration at high levels.

Acknowledgements

Author contributions

DY established the research in Yatir forest, with ER and YP establishing the thinning experiment, managed by DY and later by TK. Measurements were performed by TK, MT, SG, and YP. Data were curated by FT. Model simulations were performed by CT. TK, MT, and CT wrote the manuscript, with contributions from the other co-authors.

Appendix A. Supplementary material

Supplementary data to this article can be found online at https://doi.org/10.1016/j.foreco.2019.117573.

References

Baldocchi, D.D., Amthor, J.S., 2001. Canopy photosynthesis: history. In: Terrestrial Global Productivity. Academic Press, New York, NY, USA, pp. 9–31.
Bart, R.R., Tague, C.L., Moritz, M.A., 2016. Effect of tree-to-shrub type conversion in lower montane forests of the Sierra Nevada (USA) on streamflow, edited by J. A. Jones. PloS one 11 (8). https://doi.org/10.1371/journal.pone.0161805.
Biederman, J.A., Harpold, A.A., Gochis, D.J., Ewers, B.E., Reed, D.E., Papuga, S.A., Brooks, P.D., 2014. Increased evaporation following widespread tree mortality limits streamflow response. Water Resour. Res. 50 (7), 5395–5409.
Bréda, N., Granier, A., Aussenac, G., 1995. Effects of thinning on soil and tree water relations, transpiration and growth in an oak forest (Quercus petraea (Matt.) Liebl.). Tree Physiol. 15 (5), 295–306.
Calev, A., Zoref, C., Tzukerman, M., Moshe, Y., Zangy, E., Osem, Y., 2016. High-intensity thinning treatments in mature Pinus halepensis plantations experiencing prolonged drought. Eur. J. Forest Res. 135 (3), 551–563.
Clark, J.S., Iverson, L., Woodall, C.W., Allen, C.D., Bell, D.M., Bragg, D.C., Jackson, S.T., 2016. The impacts of increasing drought on forest dynamics, structure, and biodiversity in the United States. Glob. Change Biol. 22 (7), 2329–2352.
De las Heras, J., Moya, D., López-Serrano, F.R., Rubio, E., 2013. Carbon sequestration of naturally regenerated Aleppo pine stands in response to early thinning. New Forest. 44 (3), 457–470.
Del Campo, A.D., Fernandes, T.J., Molina, A.J., 2014. Hydrology-oriented (adaptive) silviculture in a semiarid pine plantation: how much can be modified the water cycle through forest management? Eur. J. Forest Res. 133 (5), 879–894.
Di Matteo, G., De Angelis, P., Brugnoli, E., Cherubini, P., Scarascia-Mugnozza, G., 2010. Tree-ring Δ13C reveals the impact of past forest management on water-use efficiency in a Mediterranean oak coppice in Tuscany (Italy). Ann. Forest Sci. 67 (5), 510.
Ellison, D., Futter, N.M., Bishop, K., 2012. On the forest cover–water yield debate: from demand-to supply-side thinking. Glob. Change Biol. 18 (3), 806–820.
Farley, K.A., Jobbágy, E.G., Jackson, R.B., 2005. Effects of afforestation on water yield: a global synthesis with implications for policy. Glob. Change Biol. 11 (10), 1565–1576.
Fatichi, S., Pappas, C., Ivanov, V.Y., 2016. Modeling plant–water interactions: an eco-hydrological overview from the cell to the global scale. Wiley Interdiscip. Rev. Water 3 (3), 327–368.
Fernandes, T.J., Del Campo, A.D., Herrera, R., Molina, A.J., 2016. Simultaneous assessment, through sap flow and stable isotopes, of water use efficiency (WUE) in thinned pines shows improvement in growth, tree-climate sensitivity and WUE, but not in WUEi. For. Ecol. Manage. 361, 298–308.
Forrester, D.I., Collopy, J.J., Beadle, C.L., Warren, C.R., Baker, T.G., 2012. Effect of thinning, pruning and nitrogen fertiliser application on transpiration, photosynthesis and water-use efficiency in a young Eucalyptus nitens plantation. For. Ecol. Manage.

266, 286–300.
Garcia, E.S., Tague, C.L., 2014. Climate regime and soil storage capacity interact to effect evapotranspiration in western United States mountain catchments. Hydrol. Earth Syst. Sci. Discuss. 11 (2), 2277–2319.
Garcia, E.S., Tague, C.L., Choate, J.S., 2016. Uncertainty in carbon allocation strategy and ecophysiological parameterization influences on carbon and streamflow estimates for two western US forested watersheds. Ecol. Model. 342, 19–33. https://doi.org/10.1016/j.ecolmodel.2016.09.021.
Giuggiola, A., Ogée, J., Rigling, A., Gessler, A., Bugmann, H., Treydte, K., 2016. Improvement of water and light availability after thinning at a xeric site: which matters more? A dual isotope approach. New Phytol. 210 (1), 108–121.
Goodwin, M.J., North, M.P., Zald, H.S., Hurteau, M.D., 2018. The 15-year post-treatment response of a mixed-conifer understory plant community to thinning and burning treatments. For. Ecol. Manage. 429, 617–624.
Gruenzweig, J.M., Gelfand, I., Yakir, D., 2007. Biogeochemical factors contributing to enhanced carbon storage following afforestation of a semi-arid shrubland. Biogeosciences 4, 891–904.
Grünzweig, J.M., Lin, T., Rotenberg, E., Schwartz, A., Yakir, D., 2003. Carbon sequestration in arid-land forest. Glob. Change Biol. 9 (5), 791–799.
Guardiola-Claramonte, M., Troch, P.A., Breshears, D.D., Huxman, T.E., Switanek, M.B., Durcik, M., Cobb, N.S., 2011. Decreased streamflow in semi-arid basins following drought-induced tree die-off: a counter-intuitive and indirect climate impact on hydrology. J. Hydrol. 406 (3), 225–233.
Helman, D., Lensky, I.M., Yakir, D., Osem, Y., 2017. Forests growing under dry conditions have higher hydrological resilience to drought than do more humid forests. Glob. Change Biol. 23 (7), 2801–2817.
Jackson, R.B., Jobbágy, E.G., Avissar, R., Roy, S.B., Barrett, D.J., Cook, C.W., Murray, B.C., 2005. Trading water for carbon with biological carbon sequestration. Science 310 (5756), 1944–1947.
Kariuki, M., 2008. Modelling the impacts of various thinning intensities on tree growth and survival in a mixed species eucalypt forest in central Gippsland, Victoria, Australia. Forest Ecol. Manage. 256 (12), 2007–2017.
Klein, T., Cohen, S., Paudel, I., Preisler, Y., Rotenberg, E., Yakir, D., 2016. Diurnal dynamics of water transport, storage and hydraulic conductivity in pine trees under seasonal drought. iForest-Biogeosci. Forest. 9 (5), 710.
Klein, T., Cohen, S., Yakir, D., 2011. Hydraulic adjustments underlying drought resistance of Pinus halepensis. Tree Physiol. 31 (6), 637–648.
Klein, T., Hartmann, H., 2018. Climate change drives tree mortality. Science 362 (6416) 758–758.
Klein, T., Randin, C., Körner, C., 2015. Water availability predicts forest canopy height at the global scale. Ecol. Lett. 18 (12), 1311–1320.
Klein, T., Rotenberg, E., Cohen-Hilaleh, E., Raz-Yaseef, N., Tatarinov, F., Preisler, Y., Yakir, D., 2014a. Quantifying transpirable soil water and its relations to tree water use dynamics in a water-limited pine forest. Ecohydrology 7 (2), 409–419.
Klein, T., Yakir, D., Buchmann, N., Grünzweig, J.M., 2014b. Towards an advanced assessment of the hydrological vulnerability of forests to climate change-induced drought. New phytol. 201 (3), 712–716.
Martín-Benito, D., Del Río, M., Heinrich, I., Helle, G., Canellas, I., 2010. Response of climate-growth relationships and water use efficiency to thinning in a Pinus nigra afforestation. For. Ecol. Manage. 259 (5), 967–975.
Maseyk, K.S., Lin, T., Rotenberg, E., Grünzweig, J.M., Schwartz, A., Yakir, D., 2008. Physiology–phenology interactions in a productive semi-arid pine forest. New Phytol. 178 (3), 603–616.
McDowell, N.G., Allen, C.D., 2015. Darcy's law predicts widespread forest mortality under climate warming. Nat. Clim. Change 5 (7), 669–672.
Merzer, T., 2007. The Effects of Different Vegetative Cover on the Local hydrological Balance of a Semi-Arid Afforestation. Thesis. Ben-Guryon University of the Negev.
Moreno, G., Cubera, E., 2008. Impact of stand density on water status and leaf gas exchange in Quercus ilex. For. Ecol. Manage. 254 (1), 74–84.
Moreno-Gutiérrez, C., Barbera, G.G., Nicolas, E., De Luis, M., Castillo, V.M., Martínez-Fernández, F., Querejeta, J.I., 2011. Leaf δ18O of remaining trees is affected by thinning intensity in a semiarid pine forest. Plant Cell Environ. 34 (6), 1009–1019.
Navarro-Cerrillo, R.M., Sánchez-Salguero, R., Herrera, R., Ceacero Ruiz, C.J., Moreno-Rojas, J.M., Delgado Manzanedo, R., López-Quintanilla, J., 2016. Contrasting growth and water use efficiency after thinning in mixed Abies pinsapo–Pinus pinaster–Pinus sylvestris forests. J. Forest Sci. 62 (2), 53–64.
Nunes, A., Oliveira, G., Cabral, M.S., Branquinho, C., Correia, O., 2014. Beneficial effect of pine thinning in mixed plantations through changes in the understory functional composition. Ecol. Eng. 70, 387–396.
Olivar, J., Bogino, S., Rathgeber, C., Bonnesoeur, V., Bravo, F., 2014. Thinning has a positive effect on growth dynamics and growth–climate relationships in Aleppo pine (Pinus halepensis) trees of different crown classes. Ann. Forest Sci. 71 (3), 395–404.
Peltola, H., Miina, J., Rouvinen, I., Kellomäki, S., 2002. Effect of early thinning on the diameter growth distribution along the stem of Scots pine.
Phillips, R.P., Ibanez, I., D'Orangeville, L., Hanson, P.J., Ryan, M.G., McDowell, N.G., 2016. A belowground perspective on the drought sensitivity of forests: towards improved understanding and simulation. For. Ecol. Manage. 380, 309–320. https://doi.org/10.1016/j.foreco.2016.08.043.
Ponton, S., Flanagan, L.B., Alstad, K.P., Johnson, B.G., Morgenstern, K.A.I., Kljun, N., Barr, A.G., 2006. Comparison of ecosystem water-use efficiency among Douglas-fir forest, aspen forest and grassland using eddy covariance and carbon isotope techniques. Glob. Change Biol. 12 (2), 294–310.
Porté, A., Loustau, D., 1998. Variability of the photosynthetic characteristics of mature needles within the crown of a 25-year-old Pinus pinaster. Tree Physiol. 18 (4), 223–232.
Pukkala, T., Miina, J., Palahí, M., 2002. Thinning response and thinning bias in a young

Scots pine stand.

Preisler, Y., Tatarinov, F., Grünzweig, J.M., Bert, D., Ogée, J., Wingate, L., et al., 2019. Mortality versus survival in drought-affected Aleppo pine forest depends on the extent of rock cover and soil stoniness. Funct. Ecol.

Raz-Yaseef, N., Rotenberg, E., Yakir, D., 2010a. Effects of spatial variations in soil evaporation caused by tree shading on water flux partitioning in a semi-arid pine forest. Agric. For. Meteorol. 150 (3), 454–462.

Raz-Yaseef, N., Yakir, D., Rotenberg, E., Schiller, G., Cohen, S., 2010b. Ecohydrology of a semi-arid forest: partitioning among water balance components and its implications for predicted precipitation changes. Ecohydrology 3 (2), 143–154.

Rotenberg, E., Yakir, D., 2010. Contribution of semi-arid forests to the climate system. Science 327 (5964), 451–454.

Ruano, I., Rodríguez-García, E., Bravo, F., 2013. Effects of pre-commercial thinning on growth and reproduction in post-fire regeneration of Pinus halepensis Mill. Ann. Forest Sci. 70 (4), 357–366.

Ryan, M.G., 1991. Effects of climate change on plant respiration. Ecol. Appl. 1 (2), 157–167.

Saksa, P.C., Conklin, M.H., Battles, J.J., Tague, C.L., Bales, R.C., 2017. Forest thinning impacts on the water balance of Sierra Nevada mixed-conifer headwater basins. Water Resour. Res. 53 (7), 5364–5381. https://doi.org/10.1002/2016WR019240.

Shachnovich, Y., Berliner, P.R., Bar, P., 2008. Rainfall interception and spatial distribution of throughfall in a pine forest planted in an arid zone. J. Hydrol. 349 (1), 168–177.

Shi, H., Li, L., Eamus, D., Cleverly, J., Huete, A., Beringer, J., Hutley, L., 2014. Intrinsic climate dependency of ecosystem light and water-use-efficiencies across Australian biomes. Environ. Res. Lett. 9 (10), 104002.

Simonin, K., Kolb, T.E., Montes-Helu, M., Koch, G.W., 2007. The influence of thinning on components of stand water balance in a ponderosa pine forest stand during and after extreme drought. Agric. For. Meteorol. 143 (3), 266–276.

Sohn, J.A., Gebhardt, T., Ammer, C., Bauhus, J., Häberle, K.H., Matyssek, R., Grams, T.E., 2013. Mitigation of drought by thinning: short-term and long-term effects on growth and physiological performance of Norway spruce (Picea abies). For. Ecol. Manage. 308, 188–197.

Sprintsin, M., Karnieli, A., Berliner, P., Rotenberg, E., Yakir, D., Cohen, S., 2007. The effect of spatial resolution on the accuracy of leaf area index estimation for a forest planted in the desert transition zone. Remote Sens. Environ. 109 (4), 416–428.

Sprintsin, M., Cohen, S., Maseyk, K., Rotenberg, E., Grünzweig, J., Karnieli, A., et al., 2011. Long term and seasonal courses of leaf area index in a semi-arid forest plantation. Agric. For. Meteorol. 151 (5), 565–574.

Tague, C.L., Band, L.E., 2004. RHESSys: regional hydro-ecologic simulation system-an object-oriented approach to spatially distributed modeling of carbon, water, and nutrient cycling. Earth Interact 8 (19), 1–42.

Tague, C.L., McDowell, N.G., Allen, C.D., 2013. An integrated model of environmental effects on growth, carbohydrate balance, and mortality of Pinus ponderosa forests in the Southern Rocky Mountains. PloS one 8 (11), e80286.

Tague, C., Seaby, L., Hope, A., 2009. Modeling the eco-hydrologic response of a Mediterranean type ecosystem to the combined impacts of projected climate change and altered fire frequencies. Clim. Change 93 (1–2), 137–155. https://doi.org/10.1007/s10584-008-9497-7.

Tague, C.L., Moritz, M., Hanan, E., 2019. The changing water cycle: the eco-hydrologic impacts of forest density reduction in Mediterranean (seasonally dry) regions. WIREs Water. https://doi.org/10.1002/wat2.1350.

Vesala, T., Suni, T., Rannik, Ü., Keronen, P., Markkanen, T., Sevanto, S., Ojansuu, R., 2005. Effect of thinning on surface fluxes in a boreal forest. Global Biogeochem. Cycles 19 (2).

Vicente-Serrano, S.M., Camarero, J.J., Zabalza, J., Sanguesa-Barreda, G., López-Moreno, J.I., Tague, C.L., 2015. Evapotranspiration deficit controls net primary production and growth of silver fir: implications for Circum-Mediterranean forests under forecasted warmer and drier conditions. Agric. For. Meteorol. 206, 45–54. https://doi.org/10.1016/j.agrformet.2015.02.017.

Wang, L., Caylor, K.K., Villegas, J.C., Barron-Gafford, G.A., Breshears, D.D., Huxman, T.E., 2010. Partitioning evapotranspiration across gradients of woody plant cover: assessment of a stable isotope technique. Geophys. Res. Lett. 37 (9).

Zierl, B., Bugmann, H., Tague, C.L., 2007. Water and carbon fluxes of European ecosystems: an evaluation of the ecohydrological model RHESSys. Hydrol. Process. 21 (24), 3328–3339.